JOURNAL OF MATERIALS SCIENCE **36** (2001) 3989–3996

Ultrasonic determination of the temperature and hydrostatic pressure dependences of the elastic properties of ceramic titanium diboride

S. P. DODD
Department of Physics, University of Bath, Bath BA2 7AY, UK

M. CANKURTARAN
Hacettepe University, Department of Physics, Beytepe, 06532 Ankara, Turkey

G. A. SAUNDERS
Department of Physics, University of Bath, Bath BA2 7AY, UK
E-mail: g.a.saunders@bath.ac.uk

B. JAMES
DERA, LSAB1, Chobham Lane, Chertsey, Surrey KT16 OEE, UK

Pulse-echo-overlap measurements of ultrasonic wave velocity have been used to determine the elastic stiffness moduli and related elastic properties of titanium diboride (TiB_2) ceramic samples as functions of temperature in the range 130–295 K and hydrostatic pressure up to 0.2 GPa at room temperature. TiB_2 is an elastically stiff but light ceramic: at 295 K, the longitudinal stiffness (C_L), shear stiffness (μ), adiabatic bulk modulus (B^S), Young's modulus (E) and Poisson's ratio (σ) are 612 GPa, 252 GPa, 276 GPa, 579 GPa and 0.151, respectively. The adiabatic bulk modulus B^S is in good agreement with the results of recent theoretical calculations. All elastic moduli increase with decreasing temperature and do not show any pronounced unusual effects. The results of measurements of the effects of hydrostatic pressure on the ultrasonic wave velocity have been used to determine the hydrostatic-pressure derivatives of elastic stiffnesses and the acoustic-mode Grüneisen parameters. The values determined at 295 K for the hydrostatic-pressure derivatives $(\partial C_L/\partial P)_{P=0}$, $(\partial \mu/\partial P)_{P=0}$ and $(\partial B^S/\partial P)_{P=0}$ are 7.29 ± 0.1, 2.53 ± 0.1 and 3.91 ± 0.1, respectively. The hydrostatic-pressure derivative $(\partial B^S/\partial P)_{P=0}$ of the bulk modulus of TiB_2 ceramic is found to be larger than that estimated previously from uniaxial shock-wave loading experiments. The longitudinal (γ_L), shear (γ_S), and mean (γ^{el}) acoustic-mode Grüneisen parameters of TiB_2 are positive: the zone-centre acoustic phonons stiffen under pressure in the usual way. Since the acoustic Debye temperature Θ_D (=1190 K) is very high, the shear modes provide a substantial contribution to the acoustic phonon population at room temperature. Knowledge of the elastic and nonlinear acoustic properties sheds light on the thermal properties of ceramic TiB_2.

1. Introduction

The high chemical and thermal stability of titanium diboride (TiB_2), along with its low electrical resistivity, high thermal conductivity, low thermal expansion, high melting point (2980 °C), high elastic moduli, high hardness, and relatively low density have made it an important engineering material. TiB_2 is resistive to erosion, wear and molten metals. These properties have led to a variety of technological applications, especially in high-temperature and corrosive environments, as well as considerable scientific interest (for an overview see [1]). TiB_2 ceramics find uses in a wide range of technological applications: cutting tools, light armour materials, aluminium evaporation boats, electrodes in Hall-Heroult cells and wear parts (see for instance [1]).

Titanium diboride is a compound, which crystallizes in the hexagonal structure of the AlB_2 type with interatomic bonding mainly of a covalent nature [1–4]. Despite the technological importance of TiB_2 understanding of the elastic and nonlinear acoustic properties of its ceramic form is sparse. For design purposes the elastic behaviour of TiB_2 ceramics must be evaluated as functions of temperature and pressure. Previously the elastic moduli (i.e. Young's and shear moduli and Poisson's ratio) of ceramic TiB_2 were measured at room temperature by ultrasonic [5–8] and resonance techniques [9–12]; resonance techniques were also used to determine the temperature dependences of some of the elastic moduli of TiB_2 in a range from room temperature to about 1300 K at atmospheric pressure [9, 11, 13–15].

However, with the exception of a paper [8], no work on the effects of pressure on the elastic behaviour of TiB_2 is available in the literature (see also [16]). The present high-pressure ultrasonic study of the elastic and nonlinear acoustic properties of TiB_2 has been largely motivated by the need for accurate measurements of the effects of hydrostatic pressure on the velocities of longitudinal and shear ultrasonic waves propagated in TiB_2, which are essential for design purposes in engineering applications and scientific investigations of dynamic response of the material to applied pressure or shock-waves (see, for instance [10, 17]). To assess the nonlinear acoustic properties of TiB_2 ceramic, ultrasonic wave velocities have been measured as a function of hydrostatic pressure up to 0.2 GPa at room temperature; ultrasonic wave velocity measurements on this ceramic have been extended from room temperature down to 130 K. The outcome of this experimental work has been the determination of the technological elastic stiffness moduli and related elastic properties and how they vary with temperature and hydrostatic pressure. The elastic stiffnesses of a solid determine the slopes of the acoustic-phonon dispersion curves in long-wavelength limit; their hydrostatic-pressure dependences provide information on the shift of the mode energies with compression and hence on the anharmonicity of zone-centre acoustic phonons. The present results provide intriguing physical insight into the elastic and nonlinear acoustic properties and in turn on the thermal properties of ceramic TiB_2.

2. Experimental procedures

The TiB_2 ceramic used in this work was manufactured by Cercom (USA). Scanning electron microscope images of the grain structure were taken on suitably polished and thermally etched samples (Fig. 1). The grains are randomly oriented and have a range of sizes. To obtain a measure of the average grain size, a lineal intercept analysis was performed: the intercept length for 1000 grains was measured. Actual grain sizes (d) were calculated using the expression

$$d = 1.56(L/m_f), \tag{1}$$

where L is the measured lineal intercept length and m_f is the magnification factor used in the scanning electron microscope. The factor 1.56 is an effective correction factor derived by Mendelson [18] for random slices through a model system consisting of space filling tetrakaidecahedrally shaped grains (truncated octahedrons) with a log-normal size distribution. The ceramic was considered to be single phase. This assumption is valid considering the very low secondary phase content and low porosity. X-ray diffraction data indicated the presence of a very small proportion of a secondary phase. The diffraction data also gave evidence of a slightly preferred orientation: an increase in intensity of c-axis planes and a suppression in intensity of a-axis planes, with respect to the standard intensity values, in one principal axis direction along the pressing direction and vice versa in two orthogonal directions. The grain size distribution is shown in Fig. 2. The average grain size for this TiB_2 ceramic was calculated to be 8.2 ± 5.3 μm. The sample density ρ ($=4510 \pm 10$ kgm^{-3}) was measured by Archimedes' method using acetone as a flotation fluid. The density of the sample is 99.7% of the theoretical density (4520 kgm^{-3}) of pure TiB_2. A sample, which

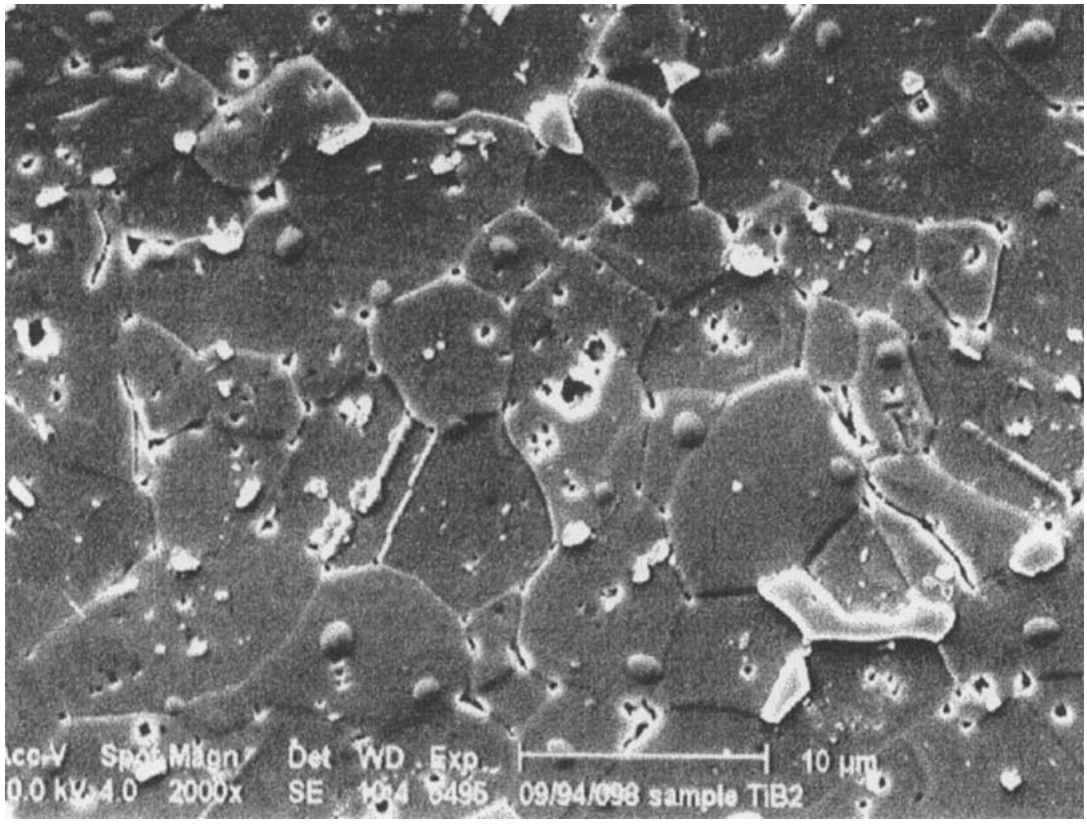

Figure 1 Scanning electron microscope images of the grain structure of TiB_2 ceramic sample.

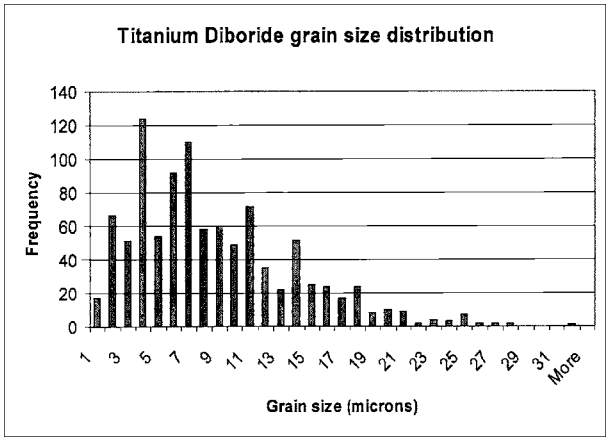

Figure 2 Grain size distribution in the TiB_2 ceramic sample. The average grain size was found to be 8.2 ± 5.3 μm.

was large enough for precision measurements of ultrasonic wave velocities, was cut and polished with a pair of faces, flat to surface irregularities of about 3 μm and parallel to better than 10^{-3} rad. The sample thickness in the direction of ultrasonic wave propagation was 9.440 ± 0.015 mm.

To generate and detect ultrasonic pulses, X- or Y-cut (for longitudinal and shear waves, respectively) 10 MHz quartz transducers, operated in the 50 MHz overtone, were bonded to the specimen using Nonaq stopcock grease for low-temperature experiments. Dow resin was used as bonding material for high-pressure experiments. Ultrasonic pulse transit times were measured using a pulse-echo-overlap system [19], capable of resolution of velocity changes to 1 part in 10^5 and particularly well suited to determination of pressure- or temperature-induced changes in ultrasound velocity. A correction was applied to the ultrasonic wave velocity for multiple reflections at the sample transducer interface [20]. The temperature dependence of ultrasound velocity was measured in the temperature ranges 130–295 K (for shear mode) and 160–295 K (for longitudinal mode) using a closed-cycle cryostat. At lower temperatures thermal expansion differences between sample, bond and transducer caused the ultrasonic signal to be lost; a number of bonding agents were tried, but none gave satisfactory results. The dependence of ultrasonic wave velocity upon hydrostatic pressure was measured at room temperature (295 K). Hydrostatic pressure up to 0.2 GPa was applied in a piston-and-cylinder apparatus using silicone oil as the pressure-transmitting medium. Pressure was measured using a pre-calibrated manganin resistance gauge. Pressure-induced changes in the sample dimensions were accounted for by using the "natural velocity (W)" technique [21].

3. Temperature dependence of the elastic stiffness moduli

The velocities of longitudinal (V_L) and shear (V_S) ultrasonic waves propagated in the TiB_2 ceramic at 295 K are given in Table I. The longitudinal velocities were measured for wave propagation direction parallel to the preferred orientation. Shear velocities were measured with their polarisation direction both parallel and perpendicular to the preferred orientation; at room temperature they differ by about 2%. The elastic parameters and temperature and pressure induced changes given in this paper are those for the shear mode for the polarisation perpendicular to principal axis. Since the ultrasonic wavelength is about two orders of magnitude larger than the average grain size, this small-grained polycrystalline ceramic can be treated as an isotropic material, which has two independent elastic stiffness moduli C_L ($=\rho V_L^2$) and μ ($=\rho V_S^2$). These elastic stiffness moduli, the adiabatic bulk modulus B^S, Young's modulus E, Poisson's ratio σ, and the acoustic Debye temperature Θ_D have been determined from the ultrasonic velocity data and sample density, using the relationships for an isotropic material (see for instance [22, 23]). The results obtained at room temperature are compared where possible in Table I with those determined previously by other researchers [8, 10, 16] for hot-pressed TiB_2 ceramic samples of similar density. There is a general agreement between the present and previous data where it exists. The small discrepancies

TABLE I The ultrasonic wave velocities, adiabatic elastic stiffness moduli and their hydrostatic-pressure derivatives, and the acoustic-mode Grüneisen parameters of ceramic TiB_2 at 295 K, in comparison with data taken from literature. The sound velocities quoted in [10] were stated to have been accurate within about 2%

Description	Present work	Ref. [10]	Ref. [8, 16]
Density ρ (kgm^{-3})	4510 ± 10	4510	4490 ± 10
Longitudinal wave velocity V_L (ms^{-1})	11650 ± 10	11210	11230 ± 210
Shear wave velocity V_s (ms^{-1})	7470 ± 10	7250	7410 ± 130
Longitudinal stiffness C_L (GPa)	612 ± 2	567	
Shear stiffness μ (GPa)	252 ± 1	237	246 ± 9
Bulk modulus B^S (GPa)	276 ± 2	251	237 ± 16
Young's modulus E (GPa)	579 ± 3	541	
Poisson's ratio σ	0.151 ± 0.002	0.141	0.114
Acoustic Debye temperature Θ_D (K)	1190 ± 5		
$(\partial C_L/\partial P)_{P=0}$	7.29 ± 0.1		(14)
$(\partial \mu/\partial P)_{P=0}$	2.53 ± 0.1		8.98 ± 0.42
$\partial B^S/\partial P)_{P=0}$	3.91 ± 0.1		2.02 ± 0.18
γ_L	1.48 ± 0.01		
γ_S	1.22 ± 0.03		
γ^{el}	1.31 ± 0.02		

may be a result of variation in microstructure and purity of the samples used in each work.

The elastic properties of anisotropic polycrystalline materials are usually dependent on microstructure. It is well known that TiB_2 has a substantial anisotropy in thermal expansion, that along the c-axis being considerably larger than that along the a-axis (see for instance [5, 11]). This anisotropy produces considerable internal stress during post-fabrication cooling and generates microcracking, relieving the localized residual stresses, when the grain size is larger than a critical size [24, 25]. The microcracking occurs in the grains and at the grain boundaries, and results in degradation of macroscopic mechanical properties [5–7]. For TiB_2, this critical grain size was found [5–7] to be about 15–20 μm. Examination of the scanning electron micrographs showed no evidence of microcracking in the hot-pressed TiB_2 ceramic used in the present work. The mean grain size is lower than the critical value and hence its elastic moduli (Table I) correspond to that of a high density, uncracked ceramic.

The value determined for Young's modulus (Table I) is somewhat larger than but comparable to those obtained [5–7, 9–11, 14, 15] for hot-pressed TiB_2; it is in good agreement with that (=569 GPa) found [26] for hot-pressed polycrystalline TiB_2 that showed no crystallographic texture. It is useful to compare the experimental values obtained for the elastic stiffness moduli of polycrystalline samples with those calculated from the single-crystal elastic constants (C_{IJ}). Only limited data at room temperature are available for the single-crystal elastic constants of TiB_2 [26, 27], since it is difficult to grow high purity, crack free, high-density single crystals of sizes suitable for ultrasonic pulse-echo measurements [28]. All the five independent elastic constants of single-crystal TiB_2 were measured [14, 15, 26] at room temperature using a mechanical resonance method. The values determined in the present work for the Young's and shear moduli of TiB_2 ceramic (Table I) are in reasonable agreement with the Hashin-Shtrikman bounds (i.e., 578–580 GPa for Young's modulus and 262–263 GPa for the shear modulus, respectively) obtained [15, 26] from single-crystal elastic constants of TiB_2. This finding is in accord with the absence of microcracks in the TiB_2 ceramic sample used in the present work. Ultrasonic attenuation values for longitudinal (<0.15 dB/cm) and shear (<0.10 dB/cm) modes at 50 MHz have been measured at room temperature. These values are so low that transducer bonding and diffraction losses must constitute a significant part of the attenuation. Hence the intrinsic losses in the ceramic are very small. This supports the observation that the sample had few microcracks and good mechanical integrity.

The adiabatic bulk modulus B^S of TiB_2 ceramic (Table I) is in good agreement with the bulk modulus (=271 GPa) derived [29] from theoretical calculations of ground state properties of TiB_2. This observation indicates that there is good bonding between the grains and a lower density of microstructural defects such as microcracks in the TiB_2 ceramic used in the present work; hence its elastic properties (Table I) can be considered as representative for polycrystalline TiB_2. However, we note that the value determined for B^S of TiB_2 ceramic is considerably larger than the bulk modulus (=240 GPa) calculated from the most recent set of data for single-crystal elastic constants of TiB_2 [14, 15, 26], using

$$B = \frac{(C_{11} + C_{12})C_{33} - 2C_{13}^2}{C_{11} + C_{12} + 2C_{33} - 4C_{13}}. \qquad (2)$$

Equation (2) gives 400 GPa for the bulk modulus of single crystal TiB_2 using the C_{IJ} data reported in [27]. A value of 416.8 GPa was estimated [30] for the bulk modulus of TiB_2 from the same set of data for C_{IJ} [27], which is not consistent with the results of most measurements.

The large value of the shear modulus of TiB_2 ceramic (Table I), which is comparable to that of the bulk modulus, indicates that TiB_2 ceramic has a large resistance to applied shear stress: TiB_2 has a high rigidity. The magnitude of Poisson's ratio found for TiB_2 ceramic (Table I) is significantly larger than those determined previously [5, 7] using ultrasonic methods and that (=0.097) obtained [11] using strain gauges. The relatively small value of Poisson's ratio implies that the interatomic bonding is not central in nature.

The acoustic Debye temperature (Table I) determined for TiB_2 ceramic in the present work is comparable with the results of some of the previous measurements of elastic constants: i. e., 952–1130 K (Ref. [31]), 1140 K (Ref. [9]) and 1170 K (Ref. [13]), and that (=960 K) determined [32] using the X-ray technique. The high acoustic Debye temperature is consistent with the high elastic stiffness and mechanical strength of the material. Debye temperature is involved in a number of physical properties including heat capacity, thermal expansion, and Debye-Waller factor. However, Debye temperatures involved in different physical properties are not strictly identical [33]. Low temperature specific heat measurements gave the values of 807 K (Ref. [34]) and 820 K (Ref. [2]) for the calorimetric Debye temperature, which is much smaller than the acoustic Debye temperature, obtained from elastic stiffness measurements on polycrystalline TiB_2. The discrepancies between the acoustic and calorimetric Debye temperatures could be due to inaccuracies in elastic stiffness and specific heat measurements.

The temperature dependences of the adiabatic longitudinal and shear elastic stiffnesses, bulk and Young's moduli of TiB_2 ceramic at atmospheric pressure are shown in Fig. 3. They were obtained from the sample density and the velocities of 50 MHz ultrasonic waves propagated in the sample as it was cycled between room temperature and the lowest temperature of measurements. Corrections on elastic moduli for sample length and density changes are expected to be negligible due to the low thermal expansion of TiB_2 [1, 5]. All elastic moduli increase with decreasing temperature and do not show any pronounced unusual effects. There was no measurable thermal hysteresis in the ultrasonic wave velocities and no irreversible effects. Thermal hysteresis effects were also absent in the temperature dependences of Young's and shear moduli measured [9] in the range from room temperature to 1300 K. The

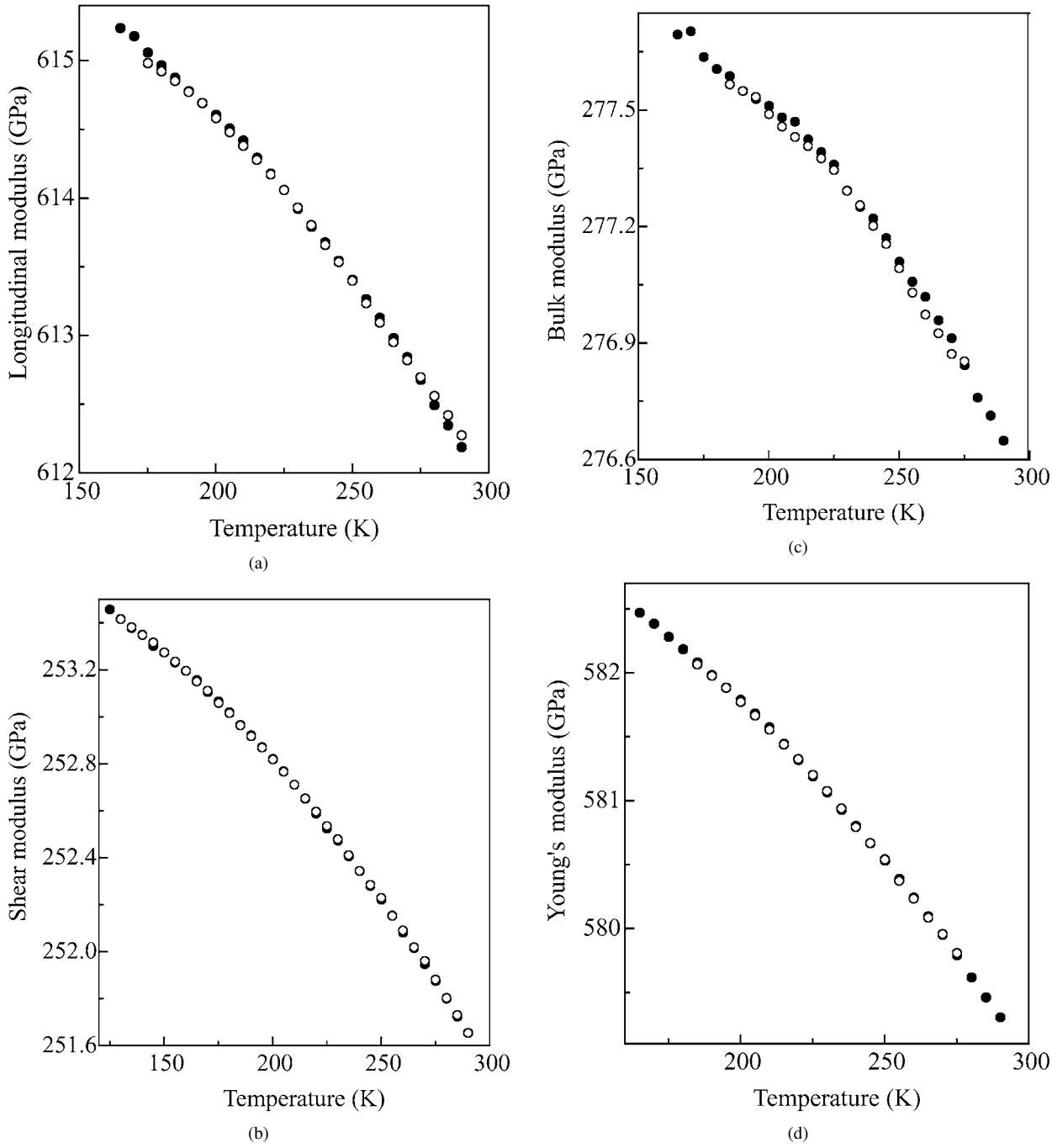

Figure 3 Temperature dependences of the adiabatic elastic moduli of TiB_2 ceramic: (a) longitudinal, (b) shear, (c) bulk modulus, and (d) Young's modulus. The filled circles correspond to measurements made with decreasing temperature and the open circles to data obtained as the temperature was increased.

acoustic Debye temperature increases smoothly with decreasing temperature in accord with stiffening of both the longitudinal and shear wave velocities. Poisson's ratio increases slightly and approximately linearly with increasing temperature. The results obtained for the temperature dependences of Young's modulus, shear modulus and Poisson's ratio are in line with and complement those reported [9, 11, 13–15] previously.

4. Hydrostatic-pressure dependences of ultrasonic wave velocity and elastic stiffness moduli

The physical properties of lightweight intermetallic compounds under pressure are of interest because of the rapidly expanding use of these materials in high-pressure and shock-wave technology [10, 16]. The effects of hydrostatic pressure on the ultrasonic wave velocity in TiB_2 ceramic are shown in Fig. 4. The data for the pressure dependence of the velocities of both longitudinal and shear ultrasonic waves are reproducible under pressure cycling and show no measurable hysteresis effects; the scatter in the data is negligible. This observation indicates that the TiB_2 ceramic does not alter in morphology under pressure cycling up to 0.2 GPa and that there is no relaxation of any residual stress. The velocities of both longitudinal and shear ultrasonic waves increase approximately linearly with pressure. This is normal behaviour: both the long-wavelength longitudinal and shear acoustic-modes stiffen under pressure, the effect on the former being much the larger.

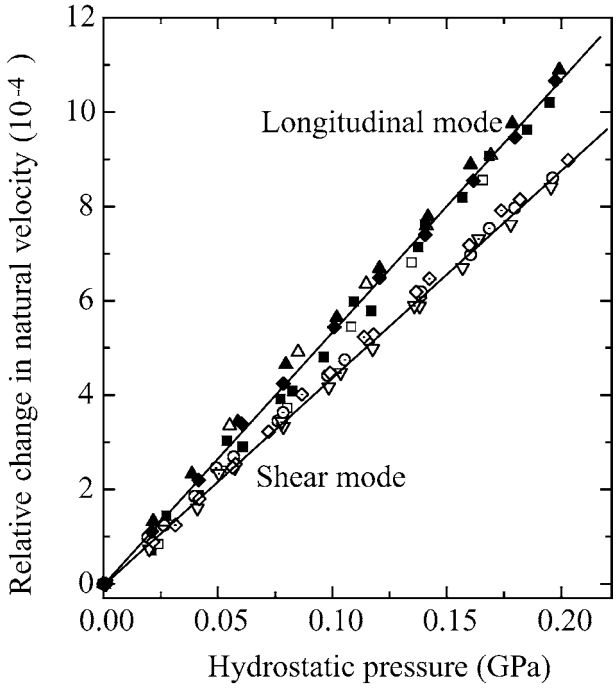

Figure 4 Hydrostatic-pressure dependence of the relative change in natural velocity for TiB_2 ceramic measured at room temperature. The filled symbols correspond to measurements made with increasing pressure and the open symbols to data as the pressure was decreased (different symbols refer to different experimental runs). The straight lines are the least-squares fits to experimental data.

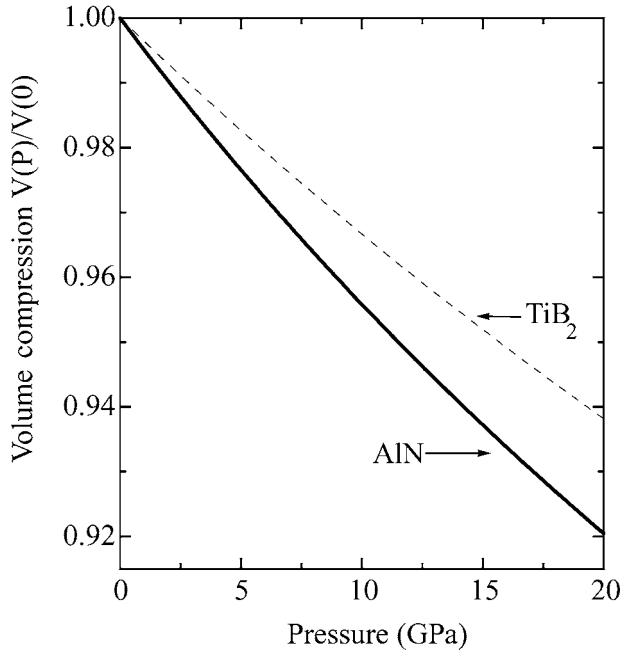

Figure 5 Volume compression of TiB_2 ceramic at room temperature (dashed line), extrapolated to very high pressures using Murnaghan's equation of state, in comparison with the results for AIN (full line).

The hydrostatic-pressure derivative $(\partial M/\partial P)_{P=0}$ of each elastic stiffness M has been obtained from the ultrasonic velocity measurements under pressure by using [35]

$$\left(\frac{\partial M}{\partial P}\right)_{P=0} = (M)_{P=0}\left[\frac{2(\partial f/\partial P)}{f} + \frac{1}{3B^T}\right]_{P=0} \quad (3)$$

where B^T is the isothermal bulk modulus, f is the pulse-echo-overlap frequency at atmospheric pressure and $\partial f/\partial P$ is its pressure derivative. The adiabatic bulk modulus B^S has been used rather than isothermal B^T throughout the calculations, a procedure, which introduces only a negligible error. The hydrostatic-pressure derivatives $(\partial C_L/\partial P)_{P=0}$, $(\partial \mu/\partial P)_{P=0}$ and $(\partial B^S/\partial P)_{P=0}$ determined for the TiB_2 ceramic have positive values (Table I) typical of a normal solid material. Both the longitudinal and shear elastic stiffnesses and thus the slopes of the corresponding acoustic-mode dispersion curves, at the long-wavelength limit, increase with pressure in the normal way. The value determined for the hydrostatic-pressure derivative $(\partial B^S/\partial P)_{P=0}$ of adiabatic bulk modulus of hot-pressed TiB_2 ceramic is larger than but comparable to those obtained by other researchers: 2.02 ± 0.18 from ultrasonic measurements [8] under pressure up to 0.7 GPa, and 1.89 ± 0.29 and 2.39 ± 0.19 deduced [16] from the compression data under uniaxial shock-wave loading reported in [10] and [36], respectively. It is worth noting that the value (=3.91) found for $(\partial B^S/\partial P)_{P=0}$ of TiB_2 ceramic is similar to the values of 3.85 and 4.0 obtained [37] for the pressure derivative of the bulk moduli of TiC and TiN single crystals, respectively, from first-principles calculations of elastic and thermal properties. Although there have been previous measurements [8] of the effects of pressure on the velocity of ultrasonic waves propagated in ceramic TiB_2, it is difficult to compare them with the present results (Table I) because the information given in [8] is not complete enough to enable calculation of the pressure derivatives of all the elastic stiffnesses with confidence. However that calculation has been made here to obtain the results shown in brackets in the last column of Table I. The present values obtained for the hydrostatic pressure derivatives of the elastic stiffnesses, which come into the normal ranges expected for a stiff ceramic, do not agree with those deduced from the data given in [8]. The values estimated for $(\partial C_L/\partial P)$ and $(\partial \mu/\partial P)$ using the data in [8] are very large for a stiff ceramic (being more representative of a soft polymer) while by contrast are inconsistent with the value quoted in [8] for $\partial B^S/\partial P$ which is rather small.

The measurements of the bulk modulus and its hydrostatic-pressure derivative have been used to calculate the volume compression $V(P)/V_0$ of TiB_2 ceramic up to very-high pressures, using an extrapolation method based on the Murnaghan's equation of state [38] in the logarithmic form. The calculation has been performed at room temperature and the results are given in Fig. 5 along with the $V(P)/V_0$ curve for AlN [39] which also has hexagonal symmetry. The TiB_2 ceramic is less compressible than AlN.

5. Grüneisen parameters and acoustic-mode vibrational anharmonicity

The hydrostatic-pressure dependences of ultrasonic wave velocities quantify to first order the vibrational anharmonicity of long-wavelength acoustic modes. Properties of a solid that depend upon thermal motion of the

atoms are much influenced by anharmonicity. Common practice is to describe the anharmonic properties in terms of Grüneisen parameters, which quantify the volume or strain dependence of the lattice vibrational frequencies. The dependence of the acoustic-mode frequency ω_p in a phonon branch p on volume V can be expressed as a mode Grüneisen parameter

$$\gamma_p = -\left[\frac{\partial(\ln \omega_p)}{\partial(\ln V)}\right]_T, \tag{4}$$

which can be obtained from the measurements of the elastic stiffnesses and their pressure derivatives. The longitudinal (γ_L) and shear (γ_S) acoustic-mode Grüneisen parameters have been determined using

$$\gamma_L = -\frac{1}{6C_L}\left[C_L - 3B^T\left(\frac{\partial C_L}{\partial P}\right)_{P=0}\right] \tag{5}$$

and

$$\gamma_S = -\frac{1}{6\mu}\left[\mu - 3B^T\left(\frac{\partial \mu}{\partial P}\right)_{P=0}\right], \tag{6}$$

respectively. The mean acoustic-mode Grüneisen parameter (γ^{el}), which is a measure of the overall contribution of zone-centre acoustic modes to the lattice vibrational anharmonicity, has been obtained using

$$\gamma^{el} = \frac{1}{3}(\gamma_L + 2\gamma_S), \tag{7}$$

which is strictly valid only at temperatures comparable with the acoustic Debye temperature. The results obtained at room temperature for γ_L, γ_S and γ^{el} of TiB_2 are included in Table I. All acoustic-mode Grüneisen parameters have normal values. From computer simulations using experimental shock-wave profiles concerning the dynamic yield strength of TiB_2, Steinberg [17] estimated a value of 1.39 for the Grüneisen gamma at room temperature and atmospheric pressure, which is in good agreement with the mean Grüneisen parameter γ^{el} (=1.31). It is also useful to note that, from first-principles calculations of elastic and thermal properties, Wolf *et al*. [37] obtained the values of 1.33 and 1.50 for the Grüneisen parameters of single crystal TiC and TiN, respectively, which are similar to γ^{el} of TiB_2 ceramic. A value of 1.1 was found [9] for the thermal Grüneisen parameter γ^{th} ($=3\alpha VB^S/C_P$) of hot-pressed TiB_2 ceramic at room temperature, which is comparable to γ_S (=1.22). Although the thermal Grüneisen parameter γ^{th} includes the effects of all phonons in the Brillouin zone, contributions from optical phonons are negligible at room temperature. Since TiB_2 has such a high acoustic Debye temperature (=1190 K), the long-wavelength acoustic phonons can be expected to dominate properties determined by vibrational anharmonicity even at room temperature. The shear acoustic-mode Grüneisen parameter γ_S is smaller than the longitudinal acoustic-mode Grüneisen parameter γ_L (Table I) accounting for the low thermal Grüneisen parameter γ^{th}. Since the acoustic Debye temperature Θ_D is very high, the shear modes play a more important role than longitudinal modes in the acoustic phonon population at room temperature. This enhances their contribution to thermal expansion and specific heat—lowering the thermal expansion and hence the thermal Grüneisen parameter.

6. Conclusions

The velocities of longitudinal and shear 50 MHz ultrasonic waves propagated in hot-pressed TiB_2 ceramic have been measured as functions of temperature and hydrostatic pressure. The TiB_2 ceramic is a stiff material elastically: its elastic stiffness moduli and acoustic Debye temperature are very large. The elastic stiffness moduli increase with decreasing temperature due to the usual vibrational anharmonicity of acoustic modes and show no unusual effects. The hydrostatic-pressure derivatives of the longitudinal and shear elastic stiffnesses and bulk modulus have positive values, hence, the long-wavelength longitudinal, shear and mean acoustic-mode Grüneisen parameters are positive. The thermal properties of TiB_2 are in accord with the low shear acoustic-mode vibrational anharmonicity.

Acknowledgments

G. A. S. and M. C. are grateful to NATO (Scientific and Environmental Affairs Division, Grant number CRG960584). B. J. is grateful to MOD for Corporate Research Programme funding. We would also like to thank E. F. Lambson, W. A. Lambson and R. C. J. Draper for technical assistance.

References

1. J. CASTAING and P. COSTA, in "Boron and Refractory Borides," edited by V. I. Matkovich (Springer-Verlag, New York, 1977) p. 390.
2. J. CASTAING, R. CAUDRON, G. TOUPANCE and P. COSTA, *Solid State Commun.* **7** (1969) 1453.
3. G. V. SAMSONOV and B. A. KOVENSKAYA, in "Boron and Refractory Borides," edited by V. I. Matkovich (Springer-Verlag, New York, 1977) p. 19.
4. K. LIE, R. BRYDSON and H. DAVOCK, *Phys. Rev. B* **59** (1999) 5361.
5. M. K. FERBER, P. F. BECHER and C. B. FINCH, *J. Amer. Ceram. Soc.* **66** (1983) C-2.
6. V. J. TENNERY, C. B. FINCH, C. S. YUST and G. W. CLARK, in "Science of Hard Materials," edited by R. K. Viswanadham (Plenum Press, New York, 1983) p. 891.
7. P. F. BECHER, C. B. FINCH and M. K. FERBER, *J. Mater. Sci. Lett.* **5** (1986) 195.
8. A. ABBATE, J. FRANKEL and D. P. DANDEKAR, in "Recent Trends in High Pressure Research," edited by A. K. Singh (Oxford, New Delhi, 1992) p. 881.
9. D. E. WILEY, W. R. MANNING and O. HUNTER JR., *J. Less-Common Metals* **18** (1969) 149.
10. W. H. GUST, A. C. HOLT and E. B. ROYCE, *J. Appl. Phys.* **44** (1973) 550.
11. H. R. BAUMGARTNER and R. A. STEIGER, *J. Amer. Ceram. Soc.* **67** (1984) 207.
12. A. BELLOSI, T. GRAZIANI, S. GUICCIARDI and A. TAMPIERI, in "Special Ceramics 9," British Ceramic Proceedings, No. 49 (Institute of Ceramics, Stoke on Trent, 1992) p. 163.
13. R. A. ANDRIEVSKI and B. U. ASANOV, *J. Mater. Sci. Lett.* **10** (1991) 147.

14. D. J. GREEN, M.-J. PAN and J. R. HELLMANN, in "Fracture Mechanics of Ceramics, Vol. 12," edited by R. C. Bradt *et al.* (Plenum Press, New York, 1996) p. 333.
15. M.-J. PAN, P. A. HOFFMAN, D. J. GREEN and J. R. HELLMAN, *J. Amer. Ceram. Soc.* **80** (1997) 692.
16. D. P. DANDEKAR and D. C. BENFANTI, *J. Appl. Phys.* **73** (1993) 673.
17. D. J. STEINBERG, *J. de Physique IV, Colloque C3, suppl. au J. de Physique III*, Vol. 1 (1991) C3-837.
18. M. I. MENDELSON, *J. Amer. Ceram. Soc.* **52** (1969) 443.
19. E. P. PAPADAKIS, *J. Acoust. Soc. Am.* **42** (1967) 1045.
20. E. KITTINGER, *Ultrasonics* **15** (1977) 30.
21. R. N. THURSTON and K. BRUGGER, *Phys. Rev.* **133** (1964) A1604.
22. L. D. LANDAU and E. M. LIFSHITZ, "Theory of Elasticity," 3rd ed. (Pergamon Press, Oxford, 1986).
23. O. L. ANDERSON, *J. Phys. Chem. Solids* **24** (1963) 909.
24. A. G. EVANS, *Acta Metall.* **26** (1978) 1845.
25. E. D. CASE, J. R. SMYTH and O. HUNTER, *J. Mater. Sci.* **15** (1980) 149.
26. P. S. SPOOR, J. D. MAYNARD, M. J. PAN, D. J. GREEN, J. R. HELLMAN and T. TANAKA, *Appl. Phys. Lett.* **70** (1997) 1959.
27. J. J. GILMAN and B. W. ROBERTS, *J. Appl. Phys.* **32** (1961) 1405.
28. V. N. GURIN and V. S. SINELNIKOVA, in "Boron and Refractory Borides," edited by V. I. Matkovich (Springer-Verlag, New York, 1977) p. 377.
29. P. E. VAN CAMP and V. E. VAN DOREN, *High Press. Res.* **13** (1995) 335.
30. S. I. WRIGHT, *J. Appl. Cryst.* **27** (1994) 794.
31. F. W. VAHLDIEK, *J. Less-Common Metals* **12** (1967) 202.
32. M. G. MIKSIC, Tech. Repr. Nr. 032-414, Polytech. Inst. Brooklyn, 1963, p. 12.
33. D. SINGH and Y. P. VARSHNI, *Phys. Rev. B* **24** (1981) 4340.
34. Y. S. TYAN, L. E. TOTH and Y. A. CHANG, *J. Phys. Chem. Solids* **30** (1969) 785.
35. R. N. THURSTON, *Proc. IEEE* **53** (1965) 1320.
36. S. P. MARSH (ed.), "LASL Shock Hugoniot Data" (University of California Press, Berkeley, 1980), p. 354.
37. W. WOLF, R. PODLOUCKY, T. ANTRETTER and F. D. FISCHER, *Philos. Mag. B* **79** (1999) 839.
38. F. D. MURNAGHAN, *Proc. Natl. Acad. Sci. USA* **30** (1944) 244.
39. S. P. DODD, M. CANKURTARAN, G. A. SAUNDERS and B. JAMES, *J. Mater. Sci.* **36** (2001) 723.

Received 18 January
and accepted 21 August 2000

Note added in proof:
Recently, an *ab initio* calculation [40] has been made of the equation of state and elastic properties of TiB_2. The theoretical values of the bulk modulus $B^S(=292 \pm 1$ GPa) and its hydrostatic-pressure derivative $(\partial B^S/\partial P)_{P=0}(=3.34 \pm 0.03)$ are in reasonable agreement with the present measured values (Table I).

40. C. A. PEROTTONI, A. S. PEREIRA and J. A. H. DA JORNADA, *J. Phys.: Condens. Matter* **12** (2000) 7205.